

## Supporting Information

### Size Dependent Surface Charge Properties of Silica Nano- Channels: Double Layer Overlap and Inlet/Outlet Effects

Tumcan Sen<sup>1</sup>, Murat Barisik<sup>1\*</sup>

<sup>1</sup>Department of Mechanical Engineering, Izmir Institute of Technology, IZMIR, 35430

\* Corresponding author E-mail: [muratbarisik@iyte.edu.tr](mailto:muratbarisik@iyte.edu.tr)

## Details of Simulations and Mathematical Model

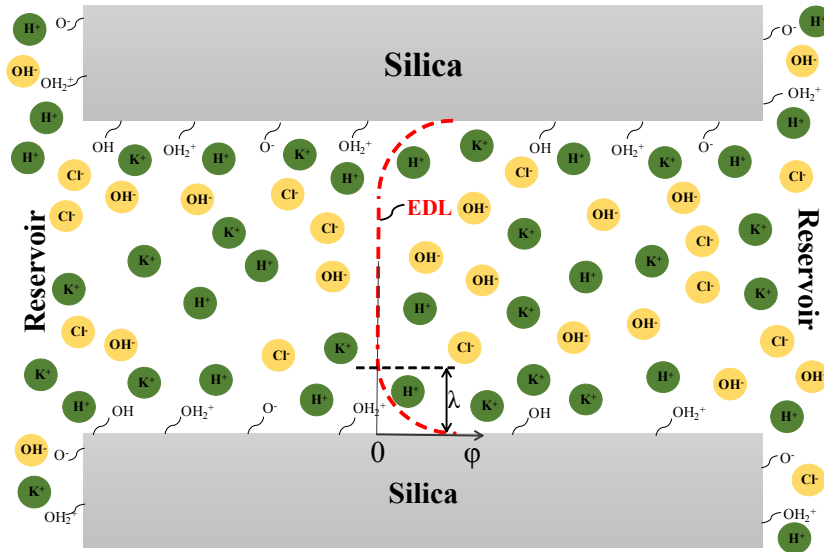


Figure S1. Schematic illustration of the solution domain consists of silica surfaces and four different ionic species.

The extension of EDL from surface is characterized by the Debye length ( $\lambda$ ) as shown in Figure S1. Debye length can be evaluated by using Equation (1).

$$\lambda = \frac{1}{\kappa} = \sqrt{\frac{\varepsilon_0 \varepsilon_r k_B T}{N_A e^2 \sum c_i z_i^2}} \quad (1)$$

Electric potential distribution within the EDL obeys the Poisson equation that is presented in Equation (2). In this equation,  $\varepsilon_0$  and  $\varepsilon_r$  are the permittivity of vacuum and dielectric constant of the aqueous solution, respectively. Dielectric constant may differ from its bulk value depending on the strength of local electric potential gradient within the double layer<sup>S1,S2</sup> but this effect may be negligible compared to the other variations in the current system. Therefore, it is treated as constant in this study.  $\psi$  is the electric potential;  $F$  is the Faraday constant;  $z_i$  and  $c_i$  are the valence and molar concentration of the  $i^{\text{th}}$  ionic species ( $i=1$  for  $\text{H}^+$ ;  $i=2$  for  $\text{K}^+$ ;  $i=3$  for  $\text{Cl}^-$ ;  $i=4$  for  $\text{OH}^-$ ) respectively.

$$-\varepsilon_0 \varepsilon_r \nabla^2 \psi = F \sum z_i c_i \quad (2)$$

Furthermore, ionic mass transport is governed by Nernst-Planck equation as shown in Equation (3). Here,  $\dot{N}_i$  is the flux density,  $D_i$  is the diffusivity, R and T are the universal gas constant and temperature, respectively. Concentrations of ionic species are maintained at their bulk values (*i.e.*  $c_i = c_{i0}$ ) at far ends of the nano-channel and no flux of ionic species is allowed through the nano-channel walls (*i.e.*  $-n \cdot \dot{N}_i = 0$ ).

$$\nabla \cdot \dot{N}_i = \nabla \cdot \left( -D_i \nabla c_i - z_i \frac{D_i}{RT} F c_i \nabla \psi \right) = 0 \quad (3)$$

Combination of Equations (2) and (3) forms the steady-state Poisson-Nernst-Planck (PNP) equations. Bulk concentration of ionic species obeys the electroneutrality condition as follows:

$$c_{10} = 10^{-pH+3} \quad c_{40} = 10^{-(14-pH)+3} \quad (4)$$

$$c_{20} = c_{KCl} \quad c_{30} = c_{KCl} + c_{10} - c_{40} \quad (5)$$

for  $pH < 7$

$$c_{20} = c_{KCl} + c_{10} - c_{40} \quad c_{30} = c_{KCl} \quad (6)$$

for  $pH > 7$

It is also important to mention that the finite ion size effects and the dispersion forces between ions and wall are neglected in the current PNP model. Further discussions on the limitations of PNP can be found in Ref S3 and Ref S4.

### Numerical Method and Validation of the Model

PNP equations in 2-D cartesian coordinates are numerically solved by finite element method with COMSOL Multiphysics. After a mesh independency study, fine structured mesh was found to be required within and at the inlet/outlet vicinity of the channel, while a coarser triangular mesh structure was adequate for the rest of the domain. The constants and parameters used in the simulations were taken as:  $\epsilon_0 \epsilon_r = 7.08 \times 10^{-10}$  F/m,  $R = 8.31$  J/(mol·K),  $F = 96485$  C/mol,  $T = 300$  K,  $N_{\text{total}} = 4.816$  1/nm<sup>2</sup>,  $pK_A = -\log K_A = 7$ , and  $pK_B = -\log K_B = 1.9$ . Moreover, the diffusivities of H<sup>+</sup>, K<sup>+</sup>, Cl<sup>-</sup> and OH<sup>-</sup> ions are set to be  $9.31 \times 10^{-9}$ ,  $1.957 \times 10^{-9}$ ,  $2.032 \times 10^{-9}$  and  $5.3 \times 10^{-9}$  m<sup>2</sup>/s, respectively.

For validation purposes, results of KCl concentrations of 10 mM and 100 mM are compared with the flat surface approximate analytical model proposed by Yeh et.al.<sup>S5</sup> In these high concentration cases, EDL fields do not overlap and the resulting surface charge density values can be described by the solution of PB. Figure S2 shows the surface charge density values for pH range from 3 to 9. The increasing trend of surface charge density with pH and KCl concentration can easily be distinguished in the figure. The current model (markers) yields identical results with the theory (lines).

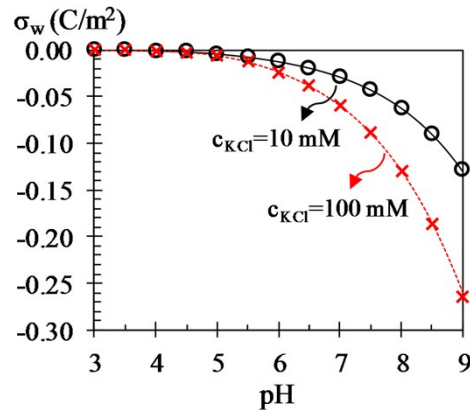


Figure S2. Surface charge densities of channel walls. Lines indicate the theoretical results while the markers are the results of the numerical model.

### Characterization of The Local and Average Surface Charge Density in Nanochannels

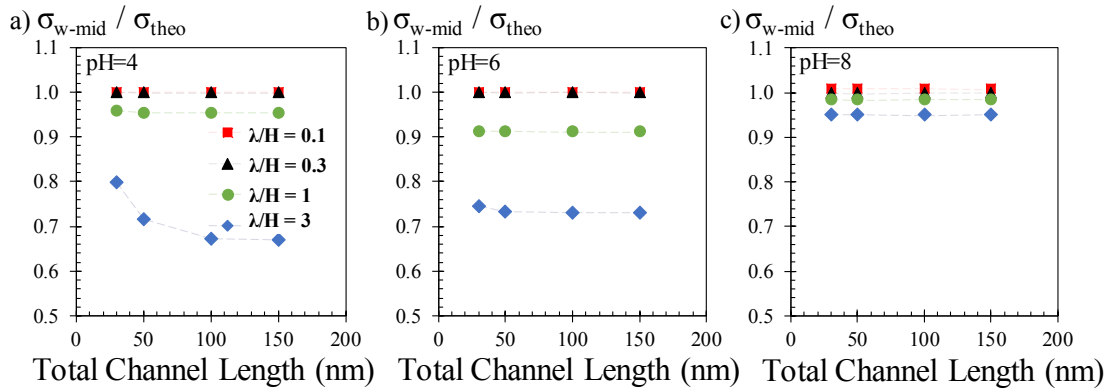


Figure S3. Silica surface charge density measured at the middle length of the different length channels. Charge values are normalized with the theoretical calculations for a flat surface.

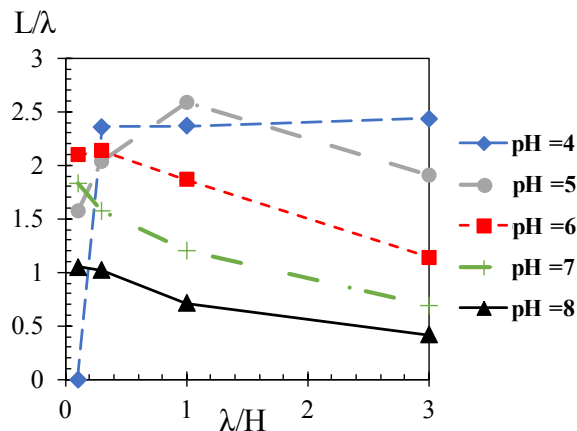


Figure S4. Entrance length values normalized by Debye length ( $\lambda$ ) of different overlapping cases for different pH values.

## References

- (S1) Zhao, H. and Zhai, S., 2013. The influence of dielectric decrement on electrokinetics. *Journal of fluid mechanics* **2013**, 724, pp.69-94.
- (S2) Qiao, R.; Aluru, N. R., Ion concentrations and velocity profiles in nanochannel electroosmotic flows. *The Journal of Chemical Physics* **2003**, 118 (10), 4692-4701.
- (S3) Wernersson, E. and Kjellander, R., On the effect of image charges and ion-wall dispersion forces on electric double layer interactions. *The Journal of chemical physics* **2006**, 125(15), 154702.
- (S4) Gavish, N., Poisson–Nernst–Planck equations with steric effects—non-convexity and multiple stationary solutions. *Physica D: Nonlinear Phenomena* **2017**, 368, 50-65
- (S5) Yeh, L.-H.; Xue, S.; Joo, S. W.; Qian, S.; Hsu, J.-P., Field Effect Control of Surface Charge Property and Electroosmotic Flow in Nanofluidics. *The Journal of Physical Chemistry C* **2012**, 116 (6), 4209-4216.